Supplementary Information

Material and Methods

DNA samples, sequencing and data mining

Blood samples from 41 individuals belonging to 16 NWm species *(Cebus xanthosternos, Cebus robustus, Cacajao melanocephalus, Chiropotes albinasus, Chiropotes utahickae, Saguinus niger, Saguinus martinsi, Saguinus bicolor, Mico humeralifer, Mico melanura, Mico saterei, Leontopithecus chrysomelas, Leontopithecus rosalia, Calimico goeldii, Cebuella pygmaea, Callithrix geofroyi)* were provided by Rio de Janeiro's Primatology Center (CPRJ). This Center is geographically located between 22°27'S-22°32'S and 42°50'W-42°56'W, in an area of 239.54 hectares with 95% of forest cover, where the animals are kept in captivity, without public access. (http://mapadecultura.rj.gov.br/guapimirim/centro-de-primatologia-do-rio-de-janeiro/). This project was registered in the official Brazilian system, which permits the collection of biological material from conservation units for research (SISBIO number 27951-2).

For some species, the DNA of more than one individual was sequenced (*OXT*: *Mico humeralifer,* n = 2; *Leontopithecus chrysomelas,* n = 2; *Leontopithecus rosalia,* n = 2; *Saguinus bicolor,* n = 3; *OXTR*: *Mico humeralifer,* n = 5; *Saguinus niger,* n = 4; *Saguinus martinsi,* n = 2; *Saguinus bicolor,* n = 4; *Cebus robustus,* n = 2; *Cebus xanthosternos,* n = 4; *Cacajao melanocephalus,* n = 2). Both *OXT* and *OXTR* DNA strands were sequenced. When changes were found, the samples were resequenced and the reading was made by a different researcher.

Due to technical difficulties in obtaining data, eventually some individuals investigated for *OXT* and *OXTR* were not the same (Table S10). Genomic DNA was extracted using the QIAamp® DNA Mini Kit (QIAGEN GmbH, Hilden, Germany) according to the protocol recommended by the manufacturer.

Primers and conditions described by Lee et al. (1) were used. *OXTR* exons were amplified using three primer sets constructed with the FastPCR software (2).

The products were purified and sequenced using Applied Biosystem 3130 or 3730 Genetic Analyzer sequencers. Sequences were aligned and their quality and accuracy evaluated using the Codon Code Aligner software (4.0 version; http://www.codoncode.com/).

GenBank accession numbers for the sequences reported here are from KM186262 to KM186289.

DNA sequences of additional species obtained from genomic databases were included in the analyses for additional species (Table S10).

Evolutionary analyses

We used the phylogeny-based maximum likelihood analysis as implemented in the CODEML program of the PAML 4.7 package to test for positive selection and/or relaxation of functional constraints (3). Two approaches which use the non-synonymous/synonymous rate ratio (dN/dS = ω), where ω < 1 indicates negative selection, ω ≅1 indicates neutral or relaxing selection, and ω > 1 indicates positive selection were applied: [a] the NsSites codon substitution model, which allows ω values to vary among sites, and [b] The Branch-site Models, which enables ω variation in different branches of the phylogeny.

For the NsSites codon substitution model, likelihood ratio tests were performed between neutral models (named M0, Neutral, M1a, Nearly Neutral, and M7, Beta) and models that identify positive selection and/or relaxation of functional constraints, named M2a (Selection, which admits three ω classes, one of which may be a value > 1); M3 (Discrete, which admits three ω classes, but never values > 1); and M8 (Beta + Selection, which admits eleven ω classes, of which one or more may be values > 1). Note that the M2a Selection model is more conservative, being less likely to lead to false positive results than M8 Beta + Selection, since it admits a lower number of ω classes (4).

The Branch-site Models approach detects positive selection acting on specific phylogenetic lineages. Maximum likelihood tests were performed between the neutral one-ratio (M1a), which assumes only one ω value for all branches, and a free-ratio model (Clade Model D), which assumes different ω parameters for each branch of the tree. We also employed the Bayes Empirical Bayes test (BEB from NsSites) or Naïve Empirical Bayes (NEB from Clade Model D) approaches, implemented in CODEML, to verify which sites could be evolving under positive selection (3-5). Additionally we used the Selecton server to visualize the sites under positive selection (6, 7).

Unrooted trees, necessary for the construction of the input files, were prepared based on the Primate phylogenetic tree provided by Perelman et al. (8), edited with PhyloWidget (9).

Coevolution, reciprocal evolutionary changes between interacting species (10), was tested using an analog definition at the molecular level (11). This interaction can be

intramolecular (within single molecules or genes) or intermolecular (between different molecules or genes) (12). Multiple sequence alignments (MSA) were used to detect correlated changes (13) in the OXT/OXTR system, considering functional and structural information. Three approaches were used. First we considered recognized specific binding sites (OXT amino acid chain positions 3 and 8; OXTR amino acid chain positions 34, 103, 209 and 284) (14-17). Second, we examined coevolutionary processes through the Bayesian Spidermonkey tool (18), available at the Datamonkey server (http://www.datamonkey.org/). Intramolecular and intermolecular OXT/OXTR analyses were performed. For the nonapeptide-receptor analysis, the OXT and OXTR sequences were concatenated. Third, we examined the pairwise comparison of *OXT*/*OXTR* divergence rates in 21 primate species to identify molecular evolutionary patterns, performed with the MEGA 5.2 Nei-Gojobori model (19).

Molecular characteristics and predicted functionality

Amino acid changes found in NWm species were compared using Grantham scores (20) as conservative (0-50), moderately conservative (51-100), moderately radical (101-150) or radical (>151) (21). Changes in physico-chemical properties (hydrophobicity, polarity, volume, chemical composition and isoelectric point) were also evaluated using PRIME (22) through the Datamonkey web server (http://www.datamonkey.org; 23) and SIFT (24).

The crystal 3D structure of the wild type oxytocin form (OXTLeu8, PDB ID: 1NPO) available in the RCSB Protein Data Bank (http://www.rcsb.org/pdb) was used to evaluate the putative impact of changes through molecular dynamics simulation. We changed the residues from those found in OXTwt using the PyMOL program (25) to obtain the oxytocin structural variants (OXT-8Pro, OXT-3Val-8Pro, OXT-8Ala, and OXT-8Thr) and AVP.

All OXT structures were independently subjected to an *in silico* molecular dynamic study for 400 nanoseconds, through the GROMACS package (v. 4.5.1 GROMOS96 53a6 force field; 26). Two simulations were performed for each system. The molecular dynamics system was created based on experimental parameters from the literature. Briefly, each oxytocin form was solvated with water (Single Point Charge model - SPC) and ions (Na^+ and Cl^-) at a physiologic concentration of 0.15M in a cubic box (≈55.60 nm^3) with at least a 9 Å solvation layer around the protein. Short-range and long-range electrostatic interactions were calculated using the cut-off and particle-mesh Ewald method (distance <1.2 nm), respectively. The system was first energy-minimized with steepest descent and conjugated gradient algorithms using an integration step

size of 2 fs. Then, the position of all heavy atoms of the protein was restricted with a force constant of 5000 kJ mol-1nm-1 during 500 ps at the temperature of 300K, to allow the molecule solvation. In the next 150 ps, the system temperature was decreased to 20K and the atom restraints were gradually removed. After that, the system was gradually heated to 300K for 1850 ps. The system was simulated with a md integrator until it reached 400 ns of simulation, keeping it coupled to an external thermal bath (v-rescale algorithm) with a τT of 0.1 ps and a pressure coupling (Parrinello-Rahman algorithm) with a τP of 2 ps. Vasopressin was also simulated using the same parameters. At the end of the simulation, all analyses were taken from the complete molecule trajectory of each peptide. Plots of the simulation were generated with the respective software from the GROMACS v4.5.1 package and visualized with xmgrace, the full-featured GUI-based Grace version (http://plasma-gate.weizmann.ac.il/Grace/).

To calculate the Free Energy Surface (FES), the values of Root Mean Square Deviation and the Radius of Gyration of each molecule along 400ns of simulation were used to retrieve low energy states. This analysis was performed using the fes.py script, developed by Birgit Strodell from the Multiscale Modelling Group (http://www.strodel.info/) and optimized by Cristóvão Freitas Iglesias Junior (http://lmdm.biof.ufrj.br/).

The clustering study, applied to obtain the most frequent conformational states of the different molecules along the simulation, was performed using the g_cluster analysis tool, from the GROMACS v4.5.1 package. The "gromos" method was employed (27), and a 0.25 nm cutoff was set.

Although 3D crystal structures of GPCRs are known, they present < 29% similarity with OXTR. This level of similarity can be used to model G protein coupled A class receptors (28, 17). However, we opted for a more conservative approach to evaluate the OXTR changes. We took into account functional information for OXTR intracellular domains (loops and C-terminal portion) to search for phosphorylation post-translational modifications, since they are very important for GPCR regulation, as well as dimerization (29, 30, 31). In order to complement this information and in order to evaluate the impact of changes in loop flexibility, we also analyzed the level of OXTR protein disorder, secondary structure, and solvent accessibility since it is well known that many GPCRs have regions of protein disorder mainly in the N-terminal region, third cytoplasmic loop and C-terminal region (32, 33). Regions of long disorder content are rich in sites for post-translational modification, protein-protein interaction and degradation sites, and, for GPCR, these sites are relevant for fine-tune signaling as well as for heteromerization (31, 34). Here we evaluated, physicochemical properties of the OXTR intracellular region, pooling

analyses of protein disorder through PONDR-FIT, secondary structure (PSIPred and NetSurfP) and solvent accessibility (NetSurfP). Prediction of the OXTR specific-kinase phosphorylation sites was performed using the consensus results from three available software packages: [a] PPSP 1.06 (Prediction of PK-specific Phosphorylation site (35) uses an Bayesian decision theory approach; [b] NetPhosK 1.0 (36), is based on neural network predictions of kinase specific eukaryotic protein phosphorylation sites; and [c] GPS 2.1 Group-based Prediction System (35) which is based on a group-based phosphorylation scoring algorithm. For predictions, only consensus sites for kinases experimentally known to interact with OXTR, namely Protein Kinase C (PKC; 37) and G protein-coupled receptor kinase (GRK; 38), were considered.

OXT/OXTR forms and ecological/social behavioral trait analyses

Several physical (body size in kg), social behavioral and ecological characteristics (activity cycle, habitat, locomotion, diet, social structure, mating system, gestation period, number of offspring, group size, reproductive maturity for females and males, and average life span) were compiled for the New World monkey species considered in the present study (Table S3). Seven of them [social structure, mating system, gestation period, number of offspring, group size, and reproductive maturity (female and male)] could directly or indirectly be connected with OXT and/or OXTR variants, based on the well known role of the OXT-OXTR system in social and reproductive behaviors (*i.e.* pair bonding and parental care). Significance associations were determined by Mann-Whitney or Fisher exact test (39). Differences were considered significant with a p value < 0.05 after Bonferroni correction.

References

1. Lee AG, Cool DR, Grunwald WC, et al. (2011) A novel form of oxytocin in New World monkeys. *Biol Lett.* 7(4):584-587.
2. Kalendar R, Lee D, Schulman AH. (2011) Java web tools for PCR, in silico PCR, and oligonucleotide assembly and analysis. *Genomics.* 98(2):137-144.
3. Yang Z. (2007) PAML 4: phylogenetic analysis by maximum likelihood. *Mol Biol Evol.* 24(8):1586-1591.
4. Anisimova M, Bielawski JP, Yang Z. (2002) Accuracy and power of bayes prediction of amino acid sites under positive selection. *Mol Biol Evol.* 19(6):950-958.
5. Bielawski JP, Yang Z. (2004) A maximum likelihood method for detecting functional divergence at individual codon sites, with application to gene family evolution. *J Mol Evol.* 59(1):121-132.
6. Stern A, Doron-Faigenboim A, Erez E, Martz E, Bacharach E, Pupko T. (2007) Selecton 2007: advanced models for detecting positive and purifying selection using a Bayesian inference approach. *Nucleic Acids Res.* 35(Web Server issue):W506-511.
7. Doron-Faigenboim A, Pupko T. (2007) A combined empirical and mechanistic codon model. *Mol Biol Evol.* 24(2):388-397.
8. Perelman P, Johnson WE, Roos C, et al. (2011) A molecular phylogeny of living primates. *PLoS Genet.* 7(3):e1001342.
9. Jordan GE, Piel WH. (2008) PhyloWidget: web-based visualizations for the tree of life. *Bioinformatics.* 24(14):1641-1642.
10. Thompson JN. (1994) *The coevolutionary process.* University of Chicago Press.
11. Atchley WR, Wollenberg KR, Fitch WM, Terhalle W, Dress AW. (2000) Correlations among amino acid sites in bHLH protein domains: an information theoretic analysis. *Mol Biol Evol.* 17(1):164-178.
12. Lovell SC, Robertson DL. (2010) An integrated view of molecular coevolution in protein-protein interactions. *Mol Biol Evol.* 27(11):2567-2575.
13. Pazos F, Valencia A. (2008) Protein co-evolution, co-adaptation and interactions. *EMBO J.* 27(20):2648-2655.
14. Chini B, Mouillac B, Balestre MN, et al. (1996) Two aromatic residues regulate the response of the human oxytocin receptor to the partial agonist arginine vasopressin. *FEBS Lett.* 397(2-3):201-206.
15. Wesley VJ, Hawtin SR, Howard HC, Wheatley M. (2002) Agonist-specific, high-affinity binding epitopes are contributed by an arginine in the N-terminus of the human oxytocin receptor. *Biochemistry.* 41(16):5086-5092.
16. Fanelli F, Barbier P, Zanchetta D, de Benedetti PG, Chini B. (1999) Activation mechanism of human oxytocin receptor: a combined study of experimental and computer-simulated mutagenesis. *Mol Pharmacol.* 56(1):214-225.
17. Slusarz R, Kaźmierkiewicz R, Giełdoń A, Lammek B, Ciarkowski J. (2001) Molecular docking-based test for affinities of two ligands toward vasopressin and oxytocin receptors. *Acta Biochim Pol.* 48(1):131-135.
18. Poon AF, Lewis FI, Frost SD, Kosakovsky Pond SL. (2008) Spidermonkey: rapid detection of co-evolving sites using Bayesian graphical models. *Bioinformatics.* 24(17):1949-1950.
19. Nei M, Gojobori T. (1986) Simple methods for estimating the numbers of synonymous and nonsynonymous nucleotide substitutions. *Mol Biol Evol.* 3(5):418-426.
20. Grantham R. (1974) Amino acid difference formula to help explain protein evolution. *Science.* 185(4154):862-864.

21. Li WH, Wu CI, Luo CC. (1985) A new method for estimating synonymous and nonsynonymous rates of nucleotide substitution considering the relative likelihood of nucleotide and codon changes. *Mol Biol Evol.* 2(2):150-174.
22. Atchley WR, Zhao J, Fernandes AD, Drüke T. (2005) Solving the protein sequence metric problem. *Proc Natl Acad Sci U S A.* 102(18):6395-6400.
23. Delport W, Poon AF, Frost SD, Kosakovsky Pond SL. (2010) Datamonkey 2010: a suite of phylogenetic analysis tools for evolutionary biology. *Bioinformatics.* 26(19):2455-2457.
24. Ng PC, Henikoff S. (2001) Predicting deleterious amino acid substitutions. *Genome Res.* 11(5):863-874.
25. *The PyMOL Molecular Graphics System* [computer program]. Version Version 1.5.0.4: Schrödinger, LLC) 2002.
26. Pronk S, Páll S, Schulz R, et al. (2013) GROMACS 4.5: a high-throughput and highly parallel open source molecular simulation toolkit. *Bioinformatics.* 29(7):845-854.
27. Xavier D, Karl G, Bernhard J, Dieter S, Wilfred F. van Gunsteren, Mark AE. (1999) *Peptide Folding: When Simulation Meets Experiment.* Vol 381999.
28. Slusarz MJ, Sikorska E, Slusarz R. Interactions of vasopressin and oxytocin receptors with vasopressin analogues substituted in position 2 with 3,3'-diphenylalanine--a molecular docking study. *J Pept Sci.* 2013)19(2):118-126.
29. Oakley RH, Laporte SA, Holt JA, Barak LS, Caron MG. (2001) Molecular determinants underlying the formation of stable intracellular G protein-coupled receptor-beta-arrestin complexes after receptor endocytosis*. *J Biol Chem.* 276(22):19452-19460.
30. Tobin AB. (2008) G-protein-coupled receptor phosphorylation: where, when and by whom. *Br J Pharmacol.* 153 Suppl 1:S167-176.
31. Woods AS, Jackson SN. (2013) How adenylate cyclase choreographs the pas de deux of the receptors heteromerization dance. *Neuroscience.* 238:335-344.
32. Agnati LF, Leo G, Genedani S, et al. (2008) Structural plasticity in G-protein coupled receptors as demonstrated by the allosteric actions of homocysteine and computer-assisted analysis of disordered domains. *Brain Res Rev.* 58(2):459-474.
33. Jaakola VP, Prilusky J, Sussman JL, Goldman A. (2005) G protein-coupled receptors show unusual patterns of intrinsic unfolding. *Protein Eng Des Sel.* 18(2):103-110.
34. Tovo-Rodrigues L, Roux A, Hutz MH, Rohde LA, Woods AS. (2014) Functional characterization of G-protein-coupled receptors: A bioinformatics approach. *Neuroscience.* 277C:764-779.
35. Xue Y, Ren J, Gao X, Jin C, Wen L, Yao X. (2008) GPS 2.0, a tool to predict kinase-specific phosphorylation sites in hierarchy. *Mol Cell Proteomics.* 7(9):1598-1608.
36. Blom N, Sicheritz-Pontén T, Gupta R, Gammeltoft S, Brunak S. (2004) Prediction of post-translational glycosylation and phosphorylation of proteins from the amino acid sequence. *Proteomics.* 4(6):1633-1649.
37. Berrada K, Plesnicher CL, Luo X, Thibonnier M. (2000) Dynamic interaction of human vasopressin/oxytocin receptor subtypes with G protein-coupled receptor kinases and protein kinase C after agonist stimulation. *J Biol Chem.* 275(35):27229-27237.
38. Hasbi A, Devost D, Laporte SA, Zingg HH. (2004) Real-time detection of interactions between the human oxytocin receptor and G protein-coupled receptor kinase-2. *Mol Endocrinol.* 18(5):1277-1286.
39. *IBM SPSS Statistics for Windows* [computer program]. Version 20.0. Armonk, NYReleased 2011.

Table S1. Low energy oxytocin and vasopressin conformers obtained from molecular dynamics (400ns)

	Conformers		
	Type I	**Type II**	**Type III**
Oxytocin (OXT)			
RMSD (nm)	0.45	0.35	0.54
Radius of Gyration (nm)	0.65	0.57	0.55
Vasopressin (AVP)			
RMSD (nm)	0.50	0.42	0.53
Radius of Gyration (nm)	0.70	0.57	0.58

Table S2. Estimated parameters under different codon substitution models through the OXT Branch-site Models[1]

	Model Clade D (free-ratio model, admit selection)				M1a (neutral)		Probability[2]
OXT Primates	Proportion	Clade 1	Clade 2	LogL	Proportion	LogL	M1a vs Clade Models
Hominidaevs other Primates	P_0=0.17970 P_1=0.70750 P_2=0.11279	ω_o=0.12119 ω_1=0.00000 ω_2=2.33044	ω_o=0.12119 ω_1=0.00000 ω_2=999.00000	-66.668.484	P_o=0.87355 P_1=0.12645 ω_o=0.01008 ω_1=1.00000	-67.090.904	Models >0.999
Cebidaevs other Primates	P_o=0.17283, P_1=0.72338 P_2=0.10379	ω_o=0.11802 ω_1=0.00000 ω_2=**125.9960**	ω_o=0.11802 ω_1=0.00000 ω_2=0.00000	-62.405.368	P_o=0.87355 P_1=0.12645 ω_o=0.01008 ω_1=1.00000	-67.090.904	**0.0368**
Pithecidaevs other Primates	P_o=0.70750 P_1=0.17970 P_2=0.11280	ω_o=0.00000 ω_1=0.12119 ω_2=2.33049	ω_o=0.00000 ω_1=0.12119 ω_2=999.00000	-66.668.515	P_o=0.87355 P_1=0.12645 ω_o=0.01008 ω_1=1.00000	-67.090.904	>0.999

[1]P= Proportion of codons in each ω class, where ω = dN/dS (non-synonymous/synonymous rate ratio); Two degrees of freedom were considered.
[2]Likelihood ratio test after Bonferroni correction.

Table S3. Ecological/social primate traits for the species considered in the present study[1]

Species	*Body size (kg)*	*Body length(mm)*	*Activity cycle*	*Habitat*	*Locomotion*	*Diet*	*Social structure*	*Mating system*	*Gestation period*	*Number of offspring*	*Group size (No)*	*Reprodutive maturity (months)* *Female*	*Male*	*Average life span (captivity) years*
Microcebus murinus	0.055	100-140	NT	TF	AB	LV/FR	OMMF	PGA	61	3	1	21	13	15
Otolemur garnettii	0.751	230-338	NT	TF	AB	FR/IN	MMMF	PGA	130	1	4	12	20	15
Tarsius syrichta	0.120	80-160	NT	TF	AB	IN/VT	MFPB	MGY	180	1	3	24	24	14
Callithrix jacchus	0.848	120-150	DI	TF	AB	OM	MFPB	MGY	148	2	7	16	13	16
Callithrix geoffroyi	0.375	190-350	DI	TF	AB	OM	MFPB	MGY/PA	160	2	9	16.5	16.5	10
Mico melanura	0.4	180-280	DI	TF	AB	FR/IN	MFPB/OFMM	MGY-PGY-PA	145	2	9	14.5	20	16
Mico saterei	0.4	195-230	DI	TF	AB	FR/IN	MFPB/OFMM	MGY-PGY-PA	145	2	9	14.5	20	12
Mico humeralifer	0.4	200-270	DI	TF	AB	OM	MFPB/OFMM	MGY-PGY-PA	140	2	9	14.5	20	12.5
Cebuella pygmaea	0.13	130-370	DI	TF	AQ	OM	MFPB/OFMM	PA/MGY	140	2	7	15	15	16
Callimico goeldii	0.626	210-234	DI	TF	AB	IN/FR/EX	MFPB	MGY	155	1	6	14	14	10
Leontopithecus chrysomelas	0.535	200-336	DI	TF	AB	OM	MFPB/OFMM	MGY	128	2	8	18	24	21.3
Leontopithecus rosalia	0.654	100-150	DI	TF	AB	OM	MFPB/OFMM	MGY	133	2	8	18	24	22
Saguinus niger	0.45	206-300	DI	TF	AB	OM	MFPB *	PA	140	2	8	21	21	11.1
Saguinus martinsi	0.475	206-300	DI	TF	AB	OM	MFPB *	PA	140	2	8	24	24	18
Saguinus bicolor	0.43	208-283	DI	TF	AB	LV/FR	OFMM	PA	145	2	8	18	24	19
Aotus nancymaae	0.788	637	NT	TF	AB	FL/FR	MFPB	MGY	133	1	10	11	11	?
Cebus robustus	3	300-560	DI	TF	AB	OM	OMMF/SD	PGA	165	1	20	48	72	44
Cebus xanthosternos	3	350-480	DI	TF	AB	OM	MMMF	PGA	165	1	19	48	72	30
Saimiri sciureus	0.925	300	DI	TF	AB	FR/IN	MMMF	PGY	165	1	55	36	65	27
Callicebus cupreus	1.12	247	DI	TF	AB	FR/IN	MFPB	MGY	150	1	5	?	?	25
Cacajao melanocephalus	3.2	365-485	DI	TF	AQ	FR/IN/SD	MMMF	MGY	180	1	25	43	43	12
Chiropotes uthaickae	2.9	327-480	DI	TF	AQ	FR/LV/IN	MMMF	PGA-MGY	135	1	24	48	48	15
Chiropotes albinasus	3	420-380	DI	TF	AQ	FR/LV/IN	MFPB / FF	MGY	142	1	44	48	48	15
Papio anubis	20	480-760	DI	SW TF	TQ	OM	MMMF	PGA	180	1	70	7.5	8.5	25.2
Macaca mulatta	8	450-640	DI	DV	AQ	OM	MMMF	PGA	165	1	90	3.2	5.7	36
Nomascus leucogenys	5.7	450-630	DI	TF	AB/BR	FR/LV	MFPB	MGY	210	1	5	6.5	7	28
Pan trogrodytes	50	635-925	DI	TF	QM/BR	OM	FF	PGA	230	1	85	11.5	13.5	60
Pongo abelii	60	1300-1800	DI	TF	AB/BR	FR/LV/IN	SD	PGA	254	1	2	12.2	19	55
Homo sapiens	65	1600-1800	DI	DV	BP	OM	VAR	VAR	280	1	VAR	168	144	65

[1]Information collected from the Animal Diversity Web (http://animaldiversity.ummz.umich.edu/). Activity cycle: DI=Diurnal; NT=Nocturnal. Habitat: TF=Tropical Forest; DV=Diverse, SW=Savanna-Wood land. Locomotion: AB=Arboreal; TQ=TerrestrialQuadruped; AQ=ArborealQuadruped; BR=Brachiator; BP=Bipedal. Diet: OM=Omnivore; FR=Fruits; LV=Leaves; SD=Seeds; IN=Insects; EX=Exudates; VT=Small vertebrates. Social structure: SD=Solitary/scattered; FF=Fission-Fusion; MMMF=MultimaleMultifemale; OMMF=One Male Multifemales; MFPB=Multi Female Pair Bonds. Mating system: PGA=Polygynandry; PGY=Polygynous; PA=Polyandrous; MGY=Monogamy; VAR=Variable. *Only one reproductive female. ? = No information available. The offspring number was defined based on the average proportion of twin and single pregnancies;this and other traits present in this table should be taken as approximations.

Table S4. Statistical correlations between ecological/social primate traits and the OXT forms

Variable	Social structure	Mating system	Gestation period	Number of offspring	Group size	Maturity female	Maturity male
Test	Fisher	Fisher	Mann-Whitney	Fisher	Mann-Whitney	Mann-Whitney	Mann-Whitney
p	0.10622	0.24469	0.05357	0.00181	0.07281	0.31407	0.27284
*p**	0.744	1	0.375	**0.013**	0.510	1	1

p, statistical significance; *p**, statistical significance after Bonferroni correction.

Table S5. Non-synonymous OXTR changes in primates

			Order	Primates																				
			Suborder	Strepsirrhini	Haplorhini																			
			Family	Galaguidae	Cebidae											Pithecidae			Cercopithecidae		Hylobatidae	Hominidae		
			Subfamily		Callithrichinae								Cebinae		Saimirinae									
Protein domain	**Nucleotide**	**Amino acid**	**Grantham Score**[1]	*Otolemurgarnettii*	*Callithrixjacchus*	*Callithrixgeoffroyi*	*Micohumeralifer*	*Cebuellapygmaea*	*Callimicogoeldii*	*Saguinus bicolor*	*Saguinusmartinsi*	*Saguinusniger*	*Cebusrobustus*	*Cebusxanthosternos*	*Saimirisciureus*	*Cacajaomelanocephalus*	*Chiropotesalbinasus*	*Chiropotesutahickae*	*Papioanubis*	*Macacamulatta*	*Nomascusleucogenys*	*Pongoabelii*	*Pan troglodytes*	*Homo sapiens*
N-terminal tail	GCG>GAG	4 Ala>Glu	107	0	0	0	0	0	0	0	0	0	0	0	0	0	0	0	1	1	0	0	0	0
	CTC>TTC	5 Leu>Phe	22	0	1	0	1	1	0	1	1	1	0	1	1	1	1	1	0	0	0	0	0	0
	GCA>GTA	6 Ala>Val	64	0	0	1	1	0	0	1	1	1	1	1	0	1	0	1	0	0	0	0	0	0
	GCC>ACC	11 Ala>Thr	58	0	0	0	0	0	0	0	0	0	0	0	0	0	0	0	1	1	0	0	0	0
	GCG>GAG	13 Ala>Glu	107	0	1	1	0	1	0	0	0	0	0	0	0	0	1	0	0	0	0	0	0	0
	GTC>ATC	**14 Val>Ile**	29	0	0	0	0	0	0	0	0	0	0	0	0	0	0	0	1	0	0	0	0	
	GTC>GCC	**14 Val>Ala**	64	0	0	0	0	0	0	0	0	0	0	0	0	0	0	0		0	0	0	0	1
	GCC>TCC	16 Ala>Ser	99	0	0	0	0	0	0	0	0	0	0	0	0	0	0	0	1	1	0	0	0	0

	CGC>TGC	19 Ala>Val	64	0	1	1	0	1	1	0	0	0	0	0	0	0	0	0	0	0	0	0	0	0
	GGG>TGG	22 Gly>Trp	184	0	0	0	0	0	0	0	0	0	0	0	0	1	0	0	0	0	0	0	0	0
	GCC>TCC	23 Ala>Ser	99	0	1	1	0	1	0	0	0	0	0	1	0	0	1	0	0	0	0	0	0	0
	AGC>CGC	**27 Ser>Arg**	110	0	1	1	1		1	1	1	1	1	1	1	1		1			1	1	1	1
	AGC>CAC	**27 Ser>His**	89	0				1									1							
	AGC>TGC	**27 Ser>Cys**	112	0															1	1				
	GCC>TCC	29 Ala>Ser	99	0	1	0	0	0	0	0	0	0	0	0	0	0	0	0	0	0	0	0	0	0
	CCG>CTG	32 Pro>Leu	98	0	0	0	0	0	0	1	0	0	0	0	0	0	0	0	0	0	0	0	0	0
	CGG>CAG	33 Arg>Gln	54	0	1	1	1	1	1	1	1	1	1	1	1	1	1	1	0	0	0	0	0	0
	AAC>GAC	35 Asn>Asp	23	0	1	1	1	1	1	1	1	1	1	1	0	1	1	1	0	0	0	0	0	0
TM1	GTG>ATA	41 Val>Ile	29	0	0	0	0	1	0	0	0	0	0	0	0	0	1	0	0	0	0	0	0	0
	TGT>TCT	47 Cys>Ser	112	0	1	1	1	1	1	1	1	1	1	1	0	1	1	1	0	0	0	0	0	0
	CTC>GTC	48 Leu>Val	32	0	0	1	1	0	0	1	1	1	1	1	0	1	0	1	0	0	0	0	0	0
	TTC>CTC	51 Phe>Leu	22	0	0	0	0	0	0	0	0	0	0	0	0	0	0	0	0	0	0	0	0	1
ICL1	ACC>ATC	66 Thr>Ile	89	0	0	0	0	0	0	0	0	0	0	0	1	0	0	0	0	0	0	0	0	0
	CAC>CAG	69 His>Gln	40	0	0	0	1	0	0	1	1	1	1	1	0	1	0	1	0	0	0	0	1	1
ECL1	TTC>TAC	103 Phe>Tyr	22	0	0	0	0	0	0	0	0	0	0	0	1	0	0	0	0	0	0	0	0	0
TM3	ATG>CTG	129 Met>Leu	15	0	1	1	1	1	1	1	1	1	1	1	1	1	1	1	1	1	1	1	1	1
ICL2	ACG>TCG	147 Thr>Ser	58	0	1	1	1	1	1	1	1	1	1	1	1	1	1	1	1	1	1	1	1	1
	CGC>AGC	149 Arg>Ser	110	0	1	1	0	1	0	0	0	0	0	1	0	0	1	0	0	0	0	0	0	0
TM4	TGG>GGG	161 Trp>Gly[2]	184	0	0	0	0	0	0	0	0	0	0	1	0	0	0	0	0	0	0	0	0	0
	CTT>TTT	162 Leu>Phe	22	0	0	0	0	0	0	0	0	0	0	0	1	0	0	0	0	0	0	0	0	0
	GCG>GTG	169 Ala>Val	64	0	1	1	1	1	1	1	1	1	1	1	1	1	1	1	0	0	0	0	0	0

	GTG>ATG	172 Val>Met	21	0	1	1	1	1	1	1	1	1	1	1	1	1	1	1	0	0	0	0	0	0
ECL2	CAG>GAG	193 Gln>Glu	29	0	1	1	1	1	1	1	1	1	1	1	0	1	1	1	0	0	0	0	0	0
	CCC>TCT	197 Pro>Ser	74	0	1	1	1	1	1	1	1	1	1	1	0	1	1	1	0	0	0	0	0	0
TM5	GCC>ACC	218 Ala>Thr	58	0	0	0	0	0	0	0	0	0	0	0	1	0	0	0	0	0	0	0	0	0
ICL3	ACC>AAC	235 Thr>Asn	65	0	0	0	0	0	0	0	0	1	0	0	0	0	0	0	0	0	0	0	0	0
	GCT>TCT	237 Ala>Ser	110	0	0	0	0	0	0	0	0	1	0	0	0	0	0	0	0	0	0	0	0	0
	CCA>GCA	238 Ala>Pro	103	0	0	0	0	0	1	0	0	0	0	0	0	0	0	0	0	0	0	0	0	0
	GCG>ACG	239 Ala>Thr	71	0	0	0	0	0	0	0	0	1	0	0	0	0	0	0	0	0	0	0	0	0
	GCG>TCG	247 Ala>Ser	110	0	0	0	0	0	0	0	0	0	1	0	0	0	0	0	0	0	0	0	0	0
	GTG>GCG	248 Val>Ala	64	0	0	0	0	0	0	0	0	0	0	0	0	0	0		1	1	1	1	1	1
	GTG>ATG	248 Val>Met	21	0	0	0	0	0	0	0	0	0	0	0	0	0	0	1						
	CTT>GTT	**249 Leu>Val**	32	0	1	1	1	1	1	1	1	1	1	1	1	1	1							
	CTT>GCT	**249 Leu>Ala**	96	0														1	1	1	1	1	1	1
	GGC>CGA	250 Gly>Arg	125	0	0	0	0	0	0	0	0	0	0	0	0	0	0	1	0	0	0	0	0	0
	GGG>GCC	**251 Gly>Ala**	60	0	1	1	1		1	1	1	1	1	1	1	1								
	GGG>ACC	**251 Gly>Thr**	59	0				1									1							
	GGG>AGG	**251 Gly>Arg**	125	0														1						
	GGG>GAT	**251 Gly>Asp**	94	0															1	1	1	1	1	1
	GGG>CCG	252 Gly>Pro	42	0	0	0	0	0	0	0	0	0	0	0	0	0	0	1	0	0	0	0	0	0
	GGG>GCG	253 Gly>Ala	125	0	0	0	0	0	0	0	0	0	1	0	0	0	0	0	0	0	0	0	0	0
	CAG>CGC	254 Gln>Arg	54	0	1	1	1	1	1	1	1	1	1	1	1	1	1	1	1	1	1	1	1	1
	GTA>ATA	**255 Val>Ile**	29	0			1			1	1	1		1		1								
	GTA>ATG	**255 Val>Met**	10	0	1	1		1	1				1		1		1	1	1	1				

	GTC>ATC	263 Val>Ile	29	0	0	0	0	1	0	0	0	0	0	0	0	0	1	0	0	0	0	0	0	0
	CTG>ATG	345 Leu>Met	21	0	0	0	0	0	0	0	0	0	0	0	0	1	1	1	0	0	0	0	0	0
C-terminal tail	TCC>GCC	349 Ser>Ala	99	0	0	0	0	0	0	0	0	0	0	0	0	0	0	0	1	1	1	1	1	1
	AGC>AGG	350 Ser>Arg	110	0	0	?	?	0	0	0	0	0	1	1	0	0	0	0	0	0	0	0	0	0
	AAG>AGG	353 Lys>Arg	26	0	0	0	0	0	0	0	0	0	0	0	0	0	0	0	0	0	0	0	1	0
	AGC>AAC	**355Ser>Asn**	46	0	1	?	?	1	1	1	1	1	1	1	1	1	1	1	1	1	1	1		
	AGC>AAA	**355 Ser>Lys**	121	0		?	?																1	
	AGC>AGA	**355 Ser>Arg**	110	0		?	?																	1
	CCC>CTG	357 Pro>Leu	98	0	1	?	?	1	1	1	1	1	1	1	1	1	1	1	1	1	1	1	1	1
	ACG>ATG	360 Thr>Met	81	0	0	?	?	0	0	0	0	0	0	0	0	0	0	0	0	0	0	1	0	0
	UUC>GCC	**362 Phe>Ala**	113	0	1	1	1	1	1	1	1	1	1	1	1	1	1	1			1	1	1	1
	UUC>ACC	**362 Phe>Thr**	103	0		?	?												1	1				
	TCG>TTG	368 Ser>Leu	145	0	0	?	?	0	0	1	1	1	0	0	0	0	0	0	0	0	0	0	0	0
	CGT>CAG	**375 Arg>Gln**	43	0	1	?	?	1	1	1	1	1												
	CGT>CAC	**375 Arg>His**	29	0		?	?						1	1	1	1	1	1	1	1	1	1	1	1
	TGC>GGC	383 Cys>Gly	159	0	0	?	?	0	0	0	0	0	0	0	0	0	0	0	0	0	0	1	0	0
	ATG>ACG	388 Met>Thr	81	0	0	?	?	0	0	0	0	0	0	0	0	0	0	0	1	1	1	0	1	1
	GTG>GCA*	**389 Val>Ala**	64	0	1	?	?	1	1	1	1	1	1	1	1	1	1	1	1	1		1	1	1
	GTG>GAG	**389 Val>Glu**	107	0		?	?														1			
	Total			0	25	21	19	26	21	25	24	27	25	27	20	25	26	27	19	18	14	15	16	17
	Unique				1				1	1		3	2	1	4	1		4	1			2	1	3

Domains: EC=Extracellular; TM=Transmembrane; IC=Intracellular. 0 indicates the allele present in the reference sequence (*Otolemurgarnettii)*, whereas 1 indicates a variant allele. In **bold** different mutations in the same amino acid site: for instance, at OXTR amino acid position 27 *Otolemurgarnetti* presents a Ser, *Cebuellapygmaea* and *Chiropotesalbinasus* a His, *Papioanubis* and *Macacamulatta* a Cys, and all others a Arg ; ? = No information available. [1]Grantham scores predicted as conservative (0-50), moderately conservative (51-100), moderately radical (101-150) or radical (>151). [2]This change promotes protein damaging according predicted by SIFT tool. PRIME tool did not detect significant differences in relation to hydrophobicity, polarity, volume, chemical composition and isoelectric properties in these OXTR forms.

Table S6. OTXR putative phosphorylation sites[1]

Species	PKC 147	PKC 149[2]	PKC 152[3]	PKC 262	PKC/GRK 362[4]	PKC/GRK 363	GRK 366	GRK 368[5]	PKC 374	PKC/GRK 378	PKC/GRK 379	PKC/GRK 382	PKC/GRK 384
Otolemurgarnettii	P		P	P		P	P	P	P	P	P	P	P
Callithrixjacchus	P	P		P		P	P	P	P	P	P	P	P
Callithrixgeoffroyi	P	P		P		P	?	?	?	?	?	?	?
Micohumeralifer	P		P	P		P	?	?	?	?	?	?	?
Cebuellapygmaea	P	P		P		P	P	P	P	P	P	P	P
Callimicogoeldii	P		P	P		P	P	P	P	P	P	P	P
Saguinus bicolor	P		P	P		P	P		P	P	P	P	P
Saguinusmartinsi	P		P	P		P	P		P	P	P	P	P
Saguinusniger	P		P	P		P	P		P	P	P	P	P
Cebusrobustus	P		P	P		P	P	P	P	P	P	P	P
Cebusxanthosternos	P	P		P		P	P	P	P	P	P	P	P
Saimirisciureus	P		P	P		P	P	P	P	P	P	P	P
Cacajaomelanocephalus	P		P	P		P	P	P	P	P	P	P	P
Chiropotesalbinasus	P	P		P		P	P	P	P	P	P	P	P
Chiropotesutahickae	P		P	P		P	P	P	P	P	P	P	P

Papioanubis	P	P	P	P	P	P	P	P	P	P	P	P
Macacamulatta	P	P	P	P	P	P	P	P	P	P	P	P
Nomascusleucogenys	P	P	P		P	P	P	P	P	P	P	P
Pongoabelii	P	P	P		P	P	P	P	P	P	P	P
Pan troglodytes	P	P	P		P	P	P	P	P	P	P	P
Homo sapiens	P	P	P		P	P	P	P	P	P	P	P

[1]PKC: protein kinase C; GRK: Gprotein-coupled receptor kinase. Numbers = OXTR amino acid sites; P = presence of a phosphorylation site.
? = Non-determined. [2]Putative new phosphorylation sites in *Callithrix*,*Cebuelapygmea, Cebusxanthosternos*, and *Chiropotesalbinasus*;[3]Loss of putative phosphorylation site in *Callithrix*genus,*Cebuelapygmea, Cebusxanthosternos*, and *Chiropotesalbinasus;*[4]Putative new phosphorylation sites in *Papioanubis* and *Macacamulatta*. [5]Loss of putative phosphorylation site in *Saguinus*.

Table S7. Estimated parameters under different OXTR codon substitution models using NSsites

Model[1]	*dN/dS*[2]	Estimated parameters[3]	Likelihood ratio test	p-*value*
M0-Neutral	0.0934	ω=0.0934	-3848.845622	
M3- Discrete	0.1334	P_o=0.81694, P_1=0.16642 (P_2=0.01664) ω_o=0.01537, ω_1=0.40250, ω_2=1	-3755.871525	<<0.0001
M1a- Nearly Neutral	0.1195	P_o=0.91198, (P_1=0.08802)	-3767.747104	
M2a- Selection	**0.1526**	(ω_o=0.03448), (ω_1=1.00000) **P_o=0.91279, P_1=0.07946, (P_2=0.00775)** **(ω_o=0.03634), (ω_1=1.00000), ω_2=5.15725**	-3760.902484	**0.00106517**
M7- Beta	0.1198	[p=0.09359 q=0.67877]	-3768.205890	3.65059e-06
M8- Beta + Selection	0.1340	[p=0.14724 q=1.52768] P_o=0.98456 (P_2=0.01544) ω_2=3.37957	-3755.685268	

[1]Neutral or nearly neutral models: M0, M1a and M7; Models that identify positive selection and/or relaxation of functional constraints: M2a, M3, and M8; M0 vs M3: chi-square with four degrees of freedom (df); M1a vs M2a: chi-square with two df; M7 vs M8: chi-square with two df; [2]dN/dS = non-synonymous/synonymous rate ratio (ω); where ω < 1 indicates negative selection, $\omega \cong 1$ indicates neutral or relaxing selection, and ω > 1 indicates positive selection; [3]Within parentheses: fixed parameters; [4]Withinbrackets: Beta parameters p and q; P= proportion of codons in each ω class.

Table S8. Comparison of several non-synonymous OXT and OXTR variants in different primate species

Bayesian posterior probabilities	Intermolecular										Intramolecular **OXTR**											
	0.56				0.80						0.81				0.54				0.55			
	OXT		**OXTR**		**OXT**				**OXTR**		**23 (N-Term)**		**149 (ICL2)**		**41 (TM1)**		**263 (ICL3)**		**340 (C-Term)**		**350 (C-Term)**	
	3		**368 (C-Term)**		**8**				**345 (ICL4)**													
Species	Ile	Val	Ser	Leu	Pro	Leu	Ala	Thr	Leu	Met	Ala	Ser	Arg	Ser	Val	Ile	Val	Ile	Leu	Phe	Ser	Arg
Otolemurgarnettii	X	-	X	-	-	X	-	-	X	-	X	-	X	-	X	-	X	-	X	-	X	-
Callithrixgeoffroyi	X	-	X	-	X	-	-	-	X	-	-	X	-	X	X	-	X	-	X	-	X	-
Callithrixjacchus	X	-	X	-	X	-	-	-	X	-	-	X	-	X	X	-	X	-	X	-	X	-
Micohumeralifer	X	-	X	-	X	-	-	-	X	-	X	-	X	-	X	-	X	-	X	-	X	-
Cebuellapigmea	X	-	X	-	X	-	-	-	X	-	-	X	-	X	-	X	-	X	X	-	X	-
Callimicogoeldii	X	-	X	-	X	-	-	-	X	-	X	-	X	-	X	-	X	-	X	-	X	-
Saguinus bicolor	-	X	-	X	X	-	-	-	X	-	X	-	X	-	X	-	X	-	X	-	X	-
Saguinusmartinsi	-	X	-	X	X	-	-	-	X	-	X	-	X	-	X	-	X	-	X	-	X	-
Saguinusniger	-	X	-	X	X	-	-	-	X	-	X	-	X	-	X	-	X	-	X	-	X	-
Cebusrobustus	X	-	X	-	X	-	-	-	X	-	X	-	X	-	X	-	X	-	-	X	-	X
Cebusxanthosternos	X	-	X	-	X	-	-	-	X	-	-	X	-	X	X	-	X	-	-	X	-	X
Saimiriscireus	X	-	X	-	X	-	-	-	X	-	X	-	X	-	X	-	X	-	X	-	X	-
Cacajaomelanocephalus	X	-	X	-	-	-	X	-	-	X	X	-	X	-	X	-	X	-	X	-	X	-
Chiropotesutahickae	X	-	X	-	-	-	X	-	-	X	X	-	X	-	X	-	X	-	X	-	X	-
Chiropotesalbinasus	X	-	X	-	-	-	-	X	-	X	-	X	-	X	-	X	-	X	X	-	X	-
Papioanubis	X	-	X	-	-	X	-	-	X	-	X	-	X	-	X	-	X	-	X	-	X	-
Macacamulatta	X	-	X	-	-	X	-	-	X	-	X	-	X	-	X	-	X	-	X	-	X	-
Nomascusleucogenys	X	-	X	-	-	X	-	-	X	-	X	-	X	-	X	-	X	-	X	-	X	-
Pongoabelii	X	-	X	-	-	X	-	-	X	-	X	-	X	-	X	-	X	-	X	-	X	-
Pan troglodytes	X	-	X	-	-	X	-	-	X	-	X	-	X	-	X	-	X	-	X	-	X	-
Homo sapiens	X	-	X	-	-	X	-	-	X	-	X	-	X	-	X	-	X	-	X	-	X	-

Table S9. Pairwise Nei-Gojobori distances for *OXT* (upper right) and *OXTR* (lower left)

OXTR \ OXT	Otolemur garnettii	Callithrix jacchus	Callithrix geoffroyi	Mico humeralifer	Cebuella pygmaea	Callimico goeldii	Saguinus bicolor	Saguinus martinsi	Saguinus niger	Cebus robustus	Cebus xanthosternos	Saimiri sciureus	Cacajao melanocephalus	Chiropotes albinasus	Chiropotes utahickae	Papio anubis	Macaca mulatta	Nomascus leucogenys	Pongo abelii	Pan troglodytes	Homo sapiens
Otolemur garnettii		0,05	0,05	0,05	0,05	0,05	0,105	0,105	0,105	0,05	0,05	0,05	0,105	0,114	0,105	0	0	0	0	0	0
Callithrix jacchus	0,035		0	0	0	0	0,05	0,05	0,05	0	0	0	0,05	0,05	0,05	0,05	0,05	0,05	0,05	0,05	0,05
Callithrix geoffroyi	0,036	0,005		0,00	0,00	0,00	0,05	0,05	0,05	0,00	0,00	0,00	0,05	0,05	0,05	0,05	0,05	0,05	0,05	0,05	0,05
Mico humeralifer	0,032	0,010	0,008		0,00	0,00	0,05	0,05	0,05	0,00	0,00	0,00	0,05	0,05	0,05	0,05	0,05	0,05	0,05	0,05	0,05
Cebuella pygmaea	0,040	0,007	0,009	0,016		0,00	0,05	0,05	0,05	0,00	0,00	0,00	0,05	0,05	0,05	0,05	0,05	0,05	0,05	0,05	0,05
Callimico goeldii	0,032	0,008	0,008	0,009	0,010		0,05	0,05	0,05	0,00	0,00	0,00	0,05	0,05	0,05	0,05	0,05	0,05	0,05	0,05	0,05
Saguinus bicolor	0,034	0,013	0,010	0,002	0,018	0,012		0,00	0,00	0,05	0,05	0,05	0,11	0,11	0,11	0,11	0,11	0,11	0,11	0,11	0,105
Saguinus martinsi	0,032	0,010	0,010	0,002	0,016	0,009	0,002		0,00	0,05	0,05	0,05	0,11	0,11	0,11	0,11	0,11	0,11	0,11	0,11	0,105
Saguinus niger	0,037	0,015	0,013	0,005	0,020	0,014	0,005	0,005		0,05	0,05	0,05	0,11	0,11	0,11	0,11	0,11	0,11	0,11	0,11	0,105
Cebus robustus	0,036	0,016	0,012	0,008	0,021	0,013	0,010	0,010	0,013		0,00	0,00	0,05	0,05	0,05	0,05	0,05	0,05	0,05	0,05	0,05
Cebus xanthosternos	0,036	0,012	0,009	0,006	0,017	0,015	0,008	0,008	0,010	0,007		0,00	0,05	0,05	0,05	0,05	0,05	0,05	0,05	0,05	0,05
Saimiri sciureus	0,029	0,017	0,020	0,016	0,023	0,016	0,019	0,016	0,021	0,020	0,020		0,05	0,05	0,05	0,05	0,05	0,05	0,05	0,05	0,05
Cacajao melanocephalus	0,034	0,014	0,012	0,003	0,019	0,013	0,006	0,006	0,008	0,009	0,007	0,017		0,05	0,00	0,11	0,11	0,11	0,11	0,11	0,105
Chiropotes albinasus	0,040	0,008	0,010	0,017	0,003	0,014	0,019	0,017	0,021	0,020	0,016	0,021	0,016		0,05	0,11	0,11	0,11	0,11	0,11	0,105
Chiropotes utahickae	0,040	0,020	0,018	0,012	0,023	0,019	0,014	0,014	0,017	0,015	0,015	0,024	0,011	0,020		0,105	0,105	0,105	0,105	0,105	0,105
Papio anubis	0,029	0,029	0,031	0,029	0,035	0,027	0,031	0,029	0,033	0,031	0,032	0,023	0,030	0,033	0,033		0,00	0,00	0,00	0,00	0
Macaca mulatta	0,028	0,028	0,030	0,027	0,033	0,026	0,030	0,027	0,032	0,030	0,031	0,022	0,029	0,032	0,032	0,001		0,00	0,00	0,00	0
Nomascus leucogenys	0,023	0,024	0,024	0,023	0,030	0,021	0,025	0,023	0,028	0,024	0,026	0,020	0,024	0,029	0,028	0,009	0,008		0,00	0,00	0
Pongo abelii	0,025	0,025	0,026	0,023	0,030	0,023	0,026	0,023	0,028	0,026	0,027	0,020	0,024	0,029	0,028	0,012	0,011	0,005		0,00	0
Pan troglodytes	0,027	0,027	0,028	0,023	0,032	0,025	0,025	0,023	0,027	0,026	0,026	0,022	0,024	0,031	0,028	0,012	0,010	0,005	0,007		0
Homo sapiens	0,026	0,029	0,030	0,025	0,035	0,027	0,028	0,025	0,030	0,028	0,029	0,023	0,026	0,033	0,030	0,014	0,013	0,007	0,009	0,005	

Genetic distances increase from blue to red. Correlation (Mantel test) between the genetic distance matrices (ρ= 0.52; p = 0.0001).

Table S10. Reference data for the original/or database material and primers used in the present study

Species	OXT	OXTR	AVP	AVPR1a
Tupaia belangeri	Lee,et al.(1)	XM_006152039.1	XM_006163955.1[c]	XM_006154152.1[c]
Microcebus murinus	ENSMICT00000013788.1[b]	ENSMICG00000002030.1[b]	NM_176854[c]	NM_001104990[c]
Otolemur garnettii	XM_003788219.1[a]	XM_003785470.1[a]	NM_213952[c]	NM_001199792[c]
Tarsius syrichta	Blat[b]	Blat[b]	XM_008047997.1[c]	XM_008074126.1[c]
Callithrix jacchus	XM_002747304.1 [b]	XM_002758625.1c	XM_002747402.1[c]	KJ641425.1[c]
*Callithrix geoffroyi**	KM186262[d]	KM186278[d]	Ren, et al. (2)	KJ641427.1-KJ641449.1[c]
*Mico melanura**	KM186263[d]	NA	NA	NA
*Mico saterei**	KM186264[d]	NA	NA	NA
*Mico humeralifer**	KM186265[d]	KM186279[d]	NA	NA
*Cebuella pygmaea**	KM186266[d]	KM186280[d]	Ren, et al. (2)	KJ641423.1-KJ641445.1[c]
*Callimico goeldii**	KM186267[d]	KM186281[d]	Ren, et al. (2)	KJ641429.1-KJ641451.1[c]
*Leontopithecus chrysomelas**	KM186268[d]	NA	NA	
*Leontopithecus rosalia**	KM186269[d]	NA	Ren, et al. (2)	KJ641430.1-KJ641452.1[c]
*Saguinus niger**	KM186270[d]	KM186284[d]	NA	NA
*Saguinus martinsi**	KM186271[d]	KM186283[d]	NA	NA
*Saguinus bicolor**	KM186272[d]	KM186282[d]	NA	NA
Aotusnancy maae	JF315861.1[b]	NA	NA	NA
*Cebus robustus**	KM186273[d]	KM186285[d]	NA	NA
*Cebus xanthosternos**	KM186274[d]	KM186286[d]	NA	NA
Saimiri sciureus	JF_315866.1[a]	JF_330026.1 a	XM_003941111.1[c]	KJ641433.1-KJ641455.1[c]
Callicebus cupreus	JF315862.1[b]	NA	Ren, et al. (2)	KJ641441.1-KJ641463.1[c]
*Cacajao melanocephalus**	KM186275[d]	KM186287[d]	NA	NA
*Chiropotes utahickae**	KM186276[d]	KM186288[d]	NA	NA
*Chiropotes albinasus**	KM186277[d]	KM186289[d]	NA	NA
Papio anubis	XM_003904999.1[b]	XM_003894143.1[b]	XM_003905000.1[c]	XM_003906711.1[c]
Macaca mulatta	XM_001115045.2[b]	NM_001044732.1[c]	XM_001115061.2[c]	XM_001116798[c]
Nomascusleucogenys	XM_003277949.2[b]	XM_003264935.2[b]	XM_003277950.1[c]	XM_003252729.2[c]
Pongo abelii	XM_001160221.3[b]	XM_001144020.3[b]	XM_002830097.2[c]	XM_002823469.1[c]
Pan trogrodytes	XM_002830099.1[a]	XM_002813482.1[b]	XM_001160259.3[c]	XM_003952135.1[c]
Homo sapiens	NM_000915.3[b]	NM_000916.3[b]	NM_000490.4[c]	NM_000706.4[c]

Information from database centers: [a]UCSC; [b]Ensembl; [c]NCBI. *,[d]Species whose DNA was sequenced in our laboratory, now reported in NCBI. NA: None available.
Primers for OXTR exon 3: A: Forward CGTAAAGGGCTCGAAGGCCG, Reverse ATGCCCACCACCTGCAAGTAC; B: Forward TGCTGTGGGACATCACCT; Reverse: TCCCAGACGCTCCACATCTG; for OXTR exon 4: Forward CTGCTGCAACCCCTGGATCTA; Reverse: AGAACACTGGACTTCCTGACCCA. The PCR cycling protocol used consisted of 30 sec for 95°C, 30 sec for 59.1°(3A); 59.6° (3B) and 61°C(4), and 40 sec at 72°C for 39 cycles. Primers and conditions for amplifications of coding OXT region were obtained from Lee et al. (1).

Reference

1. Lee AG, Cool DR, Grunwald WC, et al. A novel form of oxytocin in New World monkeys. *Biol Lett.* 2011;7(4):584-587.

2. Ren D, Chin KR, French JA. (2014) Molecular Variation in AVP and AVPR1a in New World Monkeys (Primates, Platyrrhini): Evolution and Implications for Social Monogamy. PLoS One. 9(10):e111638.

A

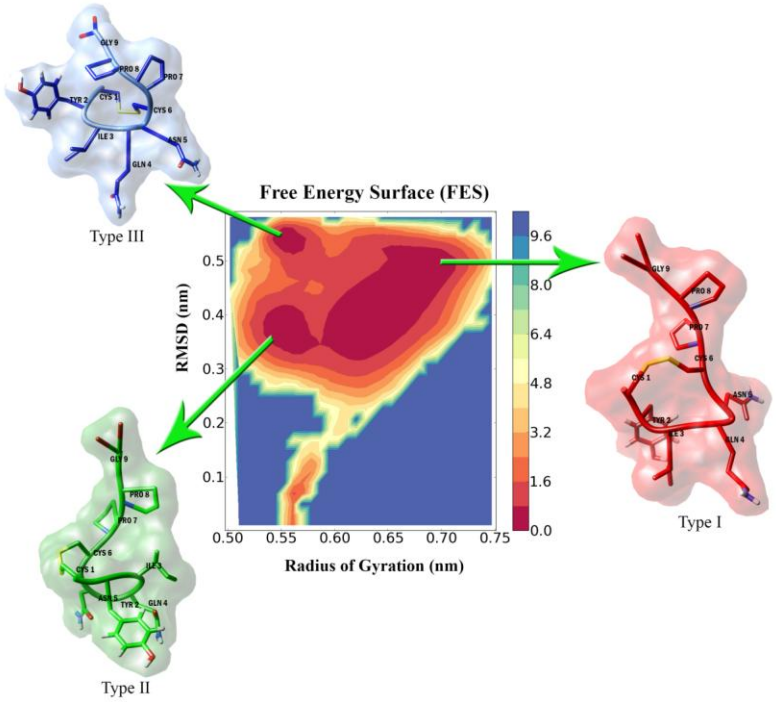

B

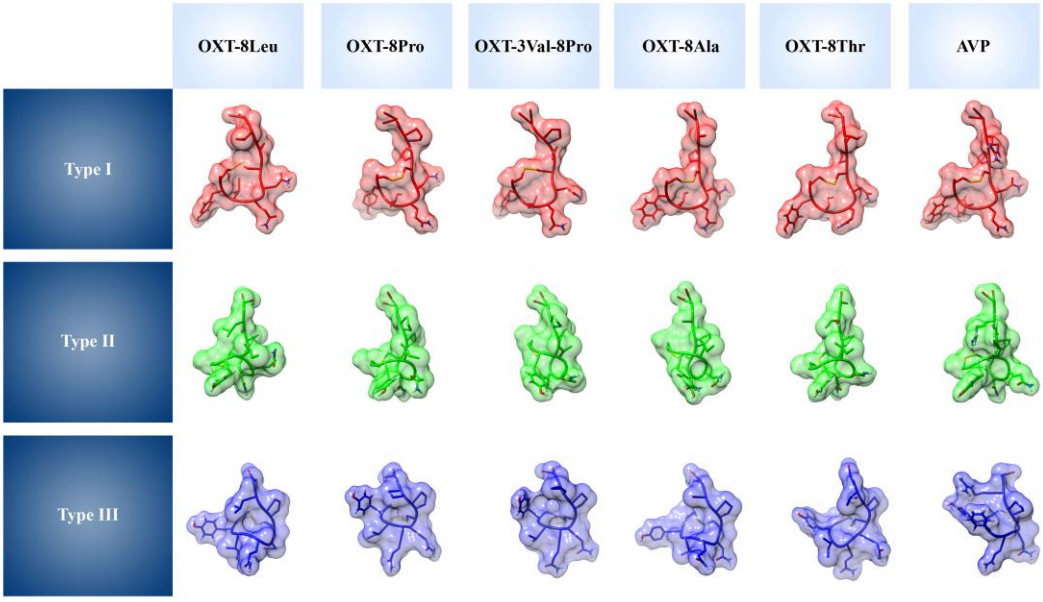

Figure S1. A) Three low energy islands oxytocin Free Energy Surface (FES) graphic, indicating its interchanging conformations observed in the simulations, for all OXT forms and AVP. The corresponding Radius of Gyration (on the x-axis) and Root Mean Square Deviation (RMSD)

values (on the y-axis) for these preferential conformers can be also observed. The free energy is color-represented with the lowest to highest values represented by warm to cool colors, respectively. The Type I (red), Type II (green) and Type III (blue) conformers are representative from each low energy island. B) Average structures of representative clusters from the three main low energy conformations (Type I, Type II and Type III) for each OXT and AVP form found in primates. The specific protein backbone pattern is shown for each conformation. Subtle differences among the molecules occur due to side chain variations, as a result of amino acid changes.

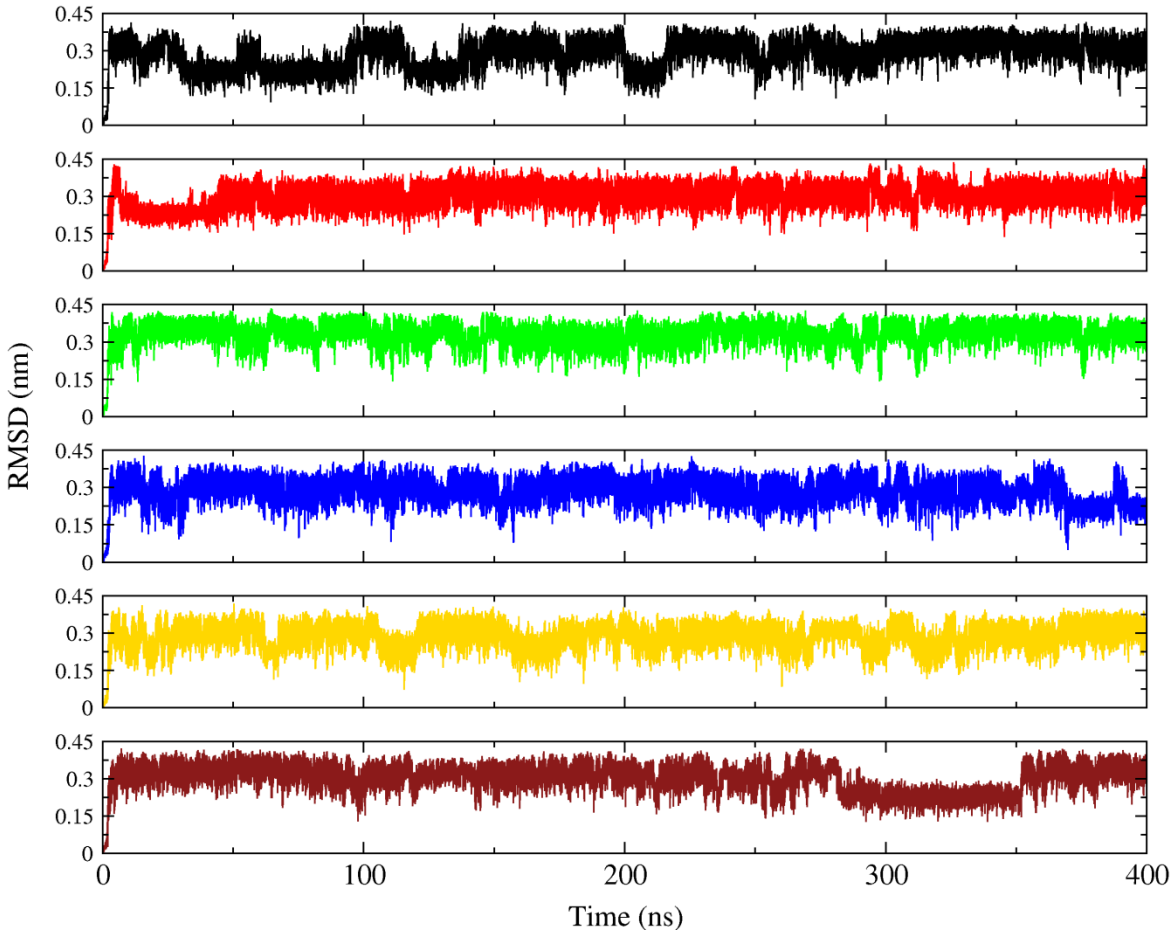

Figure S2. Root mean square deviation (RMSD) of OXTs and AVP backbone atoms over a 400ns simulation. All simulations converged at similar deviation values (around 0.3 nm).Some variation can be seen on the beginning of OXT-8Leu simulation and in the last interval of AVP simulation, for example. This indicates the presence of alternative conformers adopted by these molecules, subsequently confirmed by FES and clustering analysis. Black - OXT-8Leu; Red - OXT-8Pro; Green - OXT-3Val-8Pro; Blue - OXT-8Ala; Yellow - OXT-8Thr; Dark red - AVP.

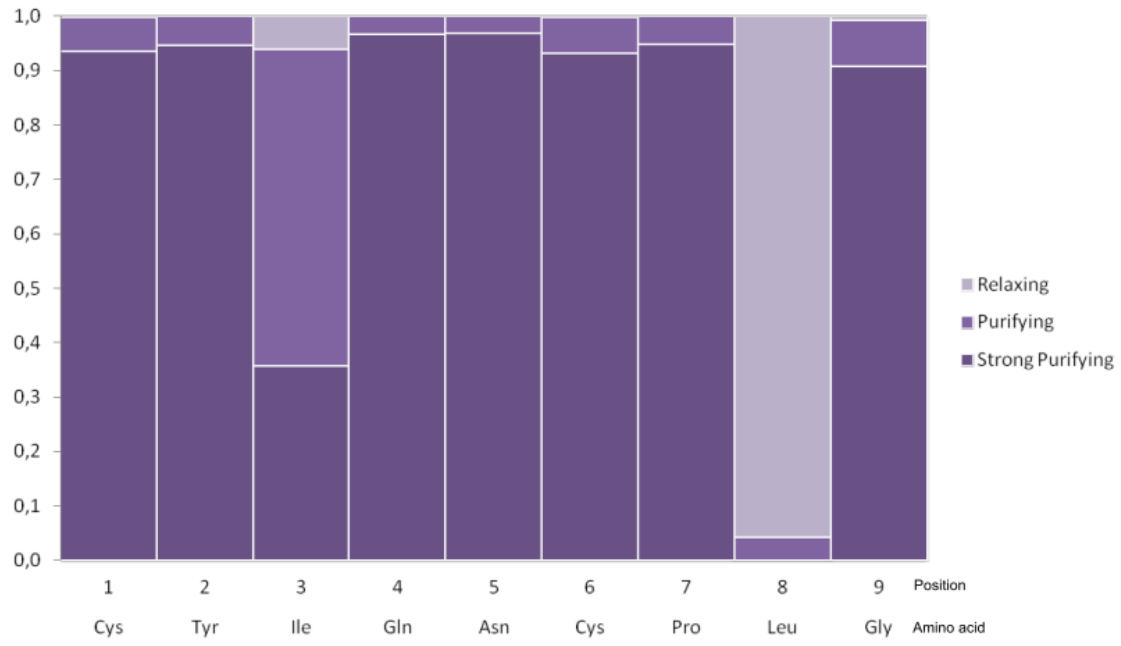

Figure S3. Posterior probabilities of the Naïve Empirical Bayes test (NEB for the BranchSites model, Clade ModelD) for each OXT amino acid position to be under strong purifying, purifying or relaxing selection. The same values were also obtained with the NsSites model.

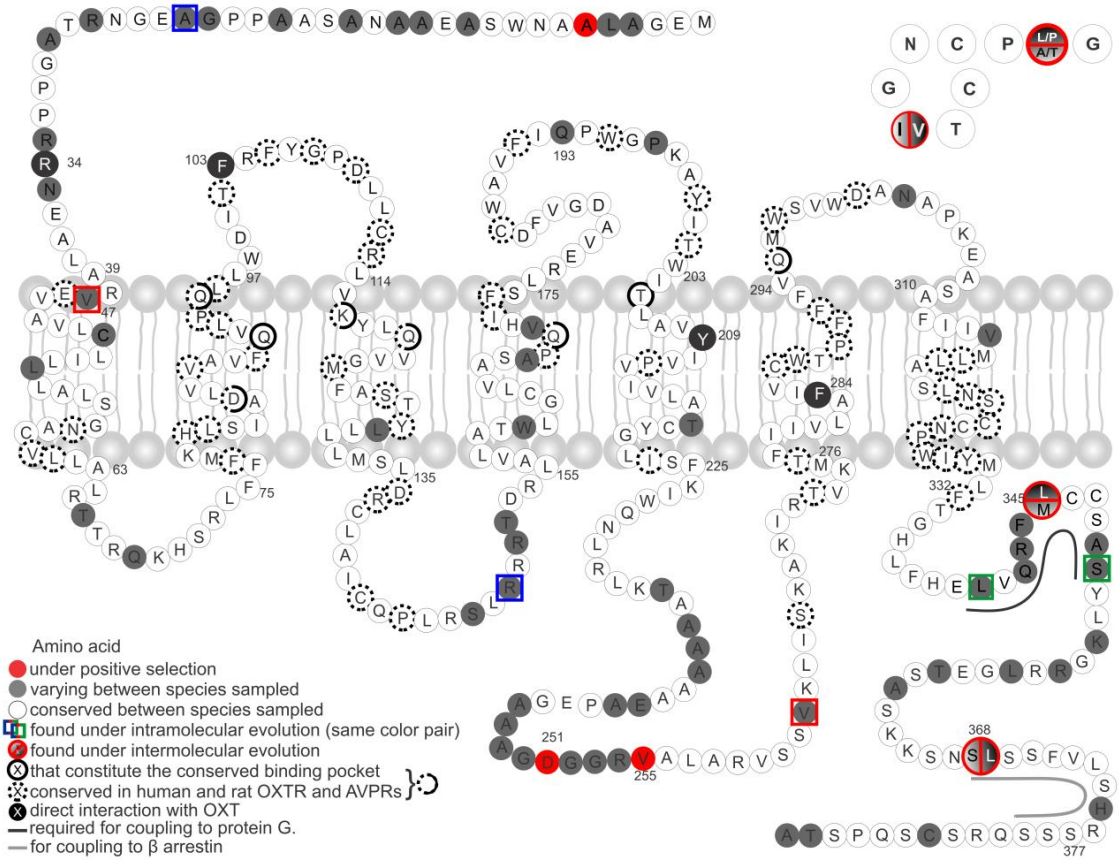

Figure S4. Snake plot of OXTR amino acid chain. Gray solid circles show interspecific variation. Amino acids in white are conserved; those in red indicate sites where positive selection was detected. White to black gradients indicate sites in which coevolution was detected. Amino acids that constitute the conserved binding pocket are solid black circles; OXTR and AVPR amino acids, which are identical in humans and rats, are shown in dotted circles. A black line indicates the amino acids required for coupling with G protein. A gray line indicates coupling-region for β arrestin. Figure includes information from the present, as well as van Kesteren and Geraertz (1), and Gimpl and Fahrenholz (2) studies. Above right, the OXT amino acid chain.

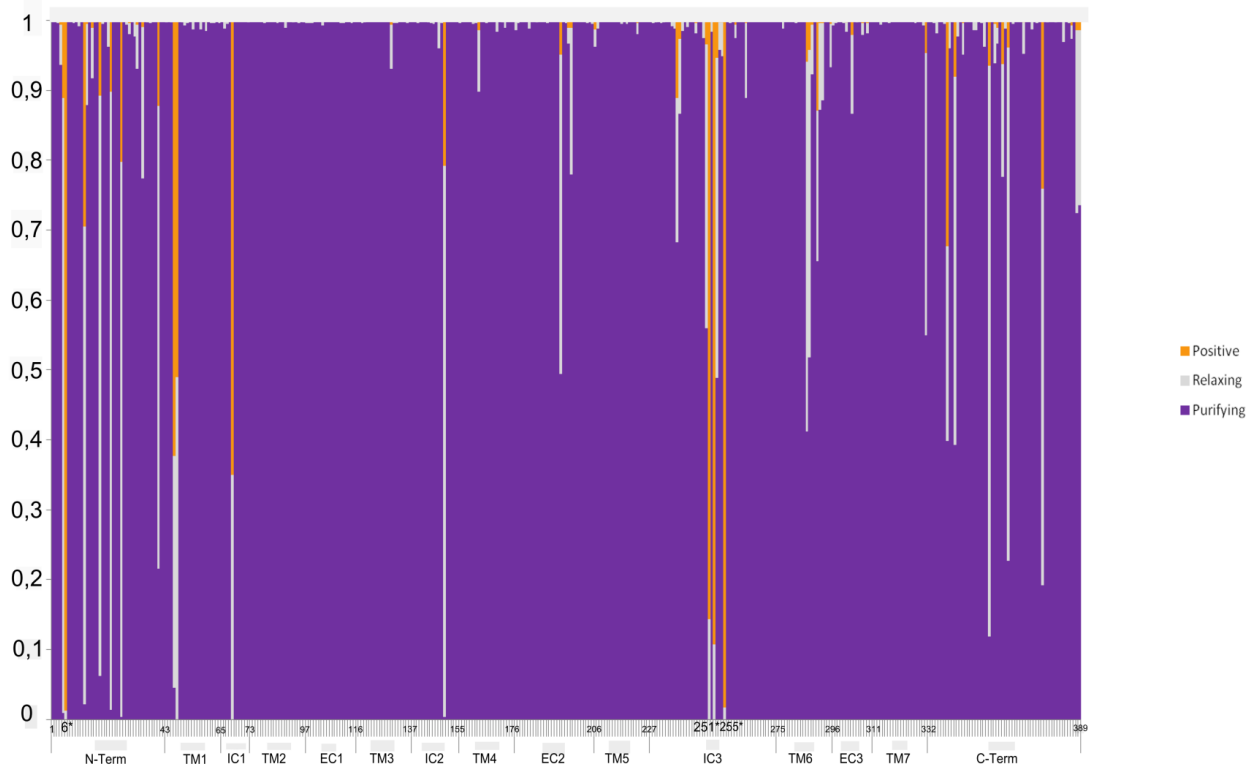

Figure S5. Posterior probabilities of Bayesian Empirical Bayes tests (BEB for NsSites; M2a-Selection model) for each OXTR amino acid position to be under purifying (purple), relaxing (grey) or positive (orange) selection.

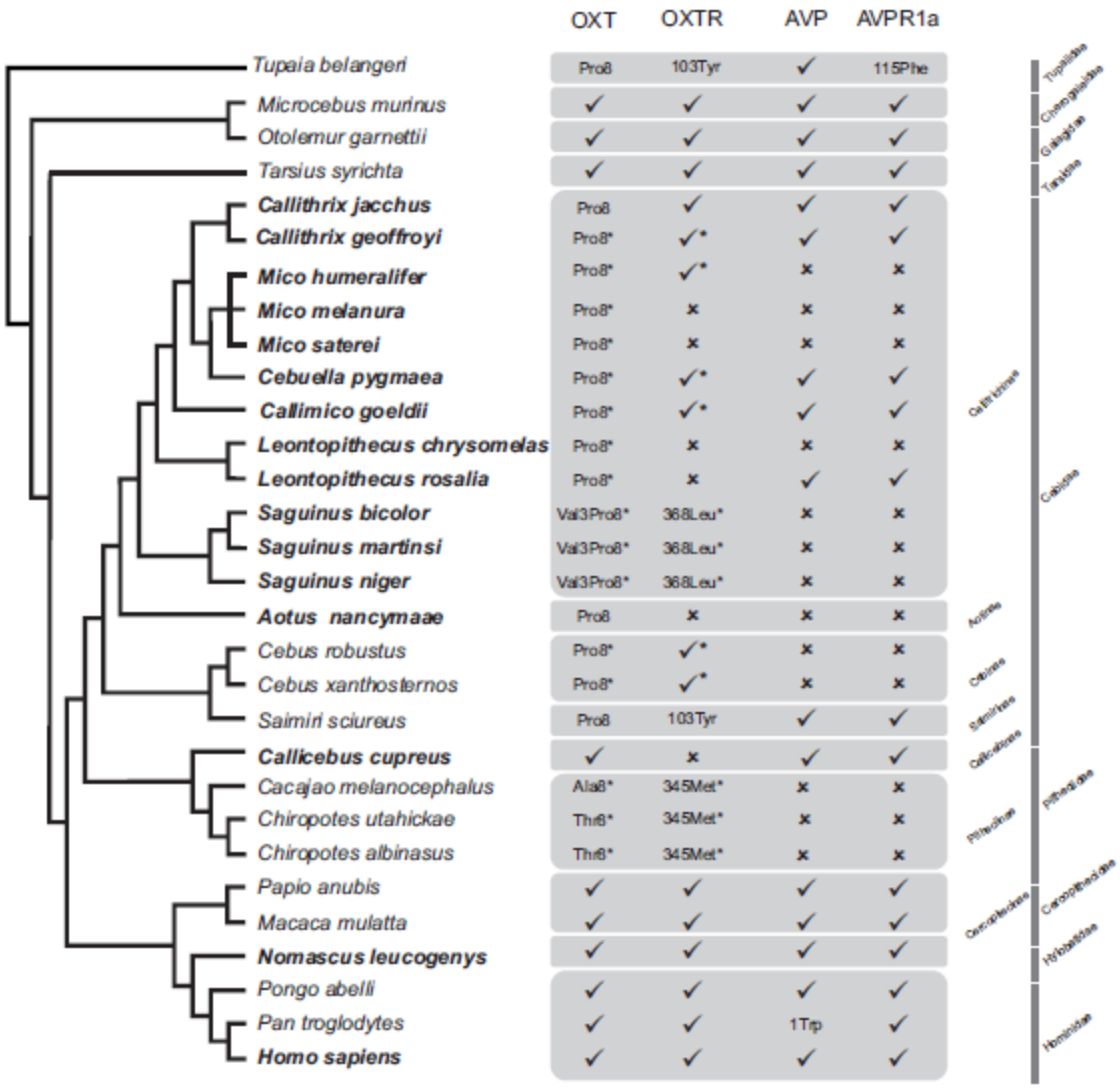

Figure S6. Nonapeptides and their receptor forms in primates. ✓indicates that the sequence is equal to human OXT (1Cys-2Tyr-3Ile-4Gln-5Asn-6Cys-7Pro-8Leu-9Gly), AVP (1Cys-2Tyr-3Phe-4Gln-5Asn-6Cys-7Pro-8Arg-9Gly); OXTR (34Arg, 103Phe, 209Tyr, 284Phe, 345Leu, 368Ser) and AVPR1a (46Arg, 115Tyr, 116Arg, 125Arg, 204Asp) at some specific positions. Phylogenetic tree based on genomic data reported by Perelman et al. (3). Taxonomic families and subfamilies are indicated, as well as species with common male care (**in bold**). Data from the present study are indicated with an asterisk, and others are from databases (Table S10). × No information available.

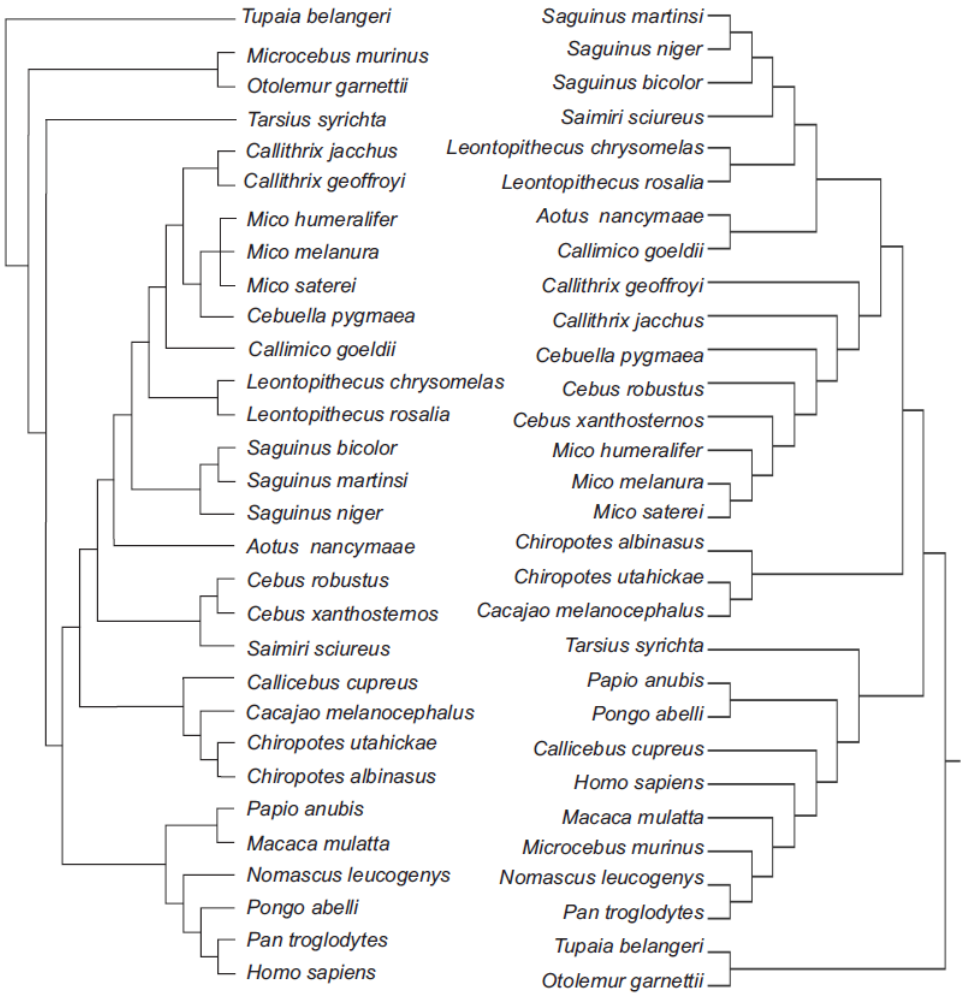

Figure S7. Comparison of the phylogenetic tree based on an ~8 Mb genomic sequence provided by Perelman et al. (3) and the *OXT* gene tree based on the sequences displayed on Figure 1.

References

1. Van Kesteren RE, Geraerts WP (1998) Molecular evolution of ligand-binding specificity in the vasopressin/oxytocin receptor family. *Ann N Y Acad Sci*. 839:25-34.

2. Gimpl G, Fahrenholz F (2001) The oxytocin receptor system: structure, function, and regulation. Physiol Rev. 81(2):629-683.

3. Perelman P, Johnson WE, Roos C, et al. (2011) A molecular phylogeny of living primates. *PLoS Genet.* 7(3):e1001342.